Heliyon 9 (2023) e13188

Contents lists available at ScienceDirect

Heliyon

journal homepage: www.cell.com/heliyon

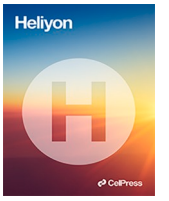

Research article

Mechanical and durability assessments of steel slag-seashell powder-based geopolymer concrete

Wilson Okoro, Solomon Oyebisi *

Department of Civil Engineering, Covenant University, P.M.B. 1023, Ota, Nigeria

ARTICLE INFO

Keywords:
Steel slag
Seashell powder
Geopolymer concrete
Compressive strength
Thermal conductivity
Materials' characterizations

ABSTRACT

Globally, an increasing carbon footprint has had a negative effect on the ecosystem and all living things. One of the sources that produces these footprints is the cement manufacturing process. Therefore, it is crucial to produce a cement substitute to reduce these footprints. The production of a geopolymer binder (GPB) is one of these possibilities. In this study, sodium silicate (Na_2SiO_3) was used as an activator in the production of geopolymer concrete (GPC) together with steel slag and oyster seashell as precursors. The materials of the concrete were prepared, cured, and tested. Workability, mechanical, durability and characterization test were conducted on the GPC. The results showed that adding a seashell increased the slump value. The optimum GPC compressive strength on a $100 \times 100 \times 100$ mm^3 cube for 3, 7, 14, 28, and 56 curing days was obtained with 10% seashell, while seashell replacement exceeded 10% declined in strength. Portland cement concrete achieved better mechanical strength when compared to steel slag seashell powder geopolymer concrete. However, steel slag seashell powder-based geopolymer gained better thermal properties than Portland cement concrete at 20% seashell replacement.

1. Introduction

Population and economic growth have led to a speedy increase in construction activities, resulting in high demand for Portland cement due to its extensive use as a binding material [1,2]. The high demand for cement is due to its primary use in concrete and mortars which are keystones in infrastructure and second only to water [3]. Cement production leads to the emission of CO_2 gas which has a negative environmental impact thus polluting the atmosphere, and increasing respiratory diseases among others [2].

The fundamental element in cement manufacture is clinker, made from the breakdown of limestone and fossil [4]. By burning fossil fuels, the limestone is heated to temperatures of 1450 °C–1500 °C. Carbonates are abundant in fossil fuels and limestone. Carbon dioxide (CO_2) gases are emitted when these carbonates are heated. The combustion of fossil fuels contributes 40–50% of the emissions, and the balance of 50–60% is to limestone heating [4–6]. A ton of Ordinary Portland cement (OPC) emits a ton of carbon dioxide (CO_2) [7]. Due to the emission of CO_2 and other greenhouse gas, it is vital to introduce an eco-friendly alternative to cement production to mitigate these emissions. Concrete is a mixture of cement, fine aggregate, and coarse aggregate that is sometimes mixed with admixtures. Geopolymer concrete has a similarity with conventional concrete but differs from cement substituted with a geopolymer binder.

Geopolymer binders are obtained by activating aluminosilicate material with alkaline solution or activators which both undergo a

* Corresponding author.
E-mail address: solomon.oyebisi@covenantuniversity.edu.ng (S. Oyebisi).

https://doi.org/10.1016/j.heliyon.2023.e13188
Received 9 September 2022; Received in revised form 17 January 2023; Accepted 19 January 2023
Available online 26 January 2023

polymeric reaction and form geopolymer paste [2]. GPCs are made from industrial by-products and agricultural by-products. Some industrial by-products are ground granulated blast furnace slag (GGBFS), condensed silica fume, waste glass, and metakaolin. In contrast, agricultural by-products are seashell powder, fly ash, rice husk ash, and corn cub ash [8–14]. The industrial and agricultural by-products are rich in alumina and silica, termed, aluminosilicate precursor. These undergo reaction with alkali activators, examples are sodium carbonate (Na_2CO_3), sodium hydroxide (NaOH), potassium hydroxide (KOH), sodium silicate (Na_2SiO_3), potassium silicate (K_2SiO_3), forming a GPB [15].

Adesanya et al. [16] stated that a two-part geopolymer (GP) is a mix design of solid powdered precursors and alkaline solution. However, it is difficult to produce geopolymers on a large scale with this method because of handling issues and the viscosity of the alkaline solutions. It is now limited to very small-scale applications. On the other hand, two-part geopolymers may be better suited to precast work, whilst one-part GP may be better suited to in situ castings [16].

The aluminosilicate precursors used in this study are oyster seashell powder and steel slag. A seashell is a hard exoskeleton that protects and supports the bodies of marine molluscs such as snails, bivalves, and chitons. The mantle, a skin-like structure in the mollusc's body wall, secretes calcium carbonate. Limestone the primary raw material in Portland cement production, has the same chemical composition as a seashell: calcium carbonate ($CaCO_3$). This certifies the possibility of a seashell as a cementitious material [3]. Seashells are the remains of mollusc, and it generates a large amount of waste [17]. Quantification of seashell waste generated globally is difficult; over 22% of worldwide aquaculture production is reported to produce sixteen million tons [18]. These waste materials are made annually and cannot be eliminated through the traditional (conventional) method [19,20]. Therefore, it is reasonable to expect that removing these waste materials and employing them as substitute materials in construction would help to address the issues of rising waste and obtaining sustainable supplemental cementitious materials [19–23].

A precursor is a substance that forms another by the reaction. Aluminosilicate precursors are industrial and agricultural waste from numerous resources, activated by an alkali (base) which depends on their chemical composition primarily on calcium, aluminium, silicon and sodium on a high percentage than the remaining chemical composition they possess. Some precursors result in calcium alumina silicate hydrate (C–A–S–H) gel, while some as sodium alumina silicate hydrate (N–A–S–H) gel due to their chemical composition. An example of raw material rich in calcium is slag which results in calcium alumina silicate hydrate (C–A–S–H) gel which possesses a tobermorite-like structure when activated due to the chemical composition system, while sodium alumina silicate hydrate (N–A–S–H) gel has low calcium content but high sodium content which possess a disordered pseudo zeolitic structure which is highly crossed linked [3]. These precursors are deployed in the formation of geopolymer which can be utilized as a binder and a concrete termed geopolymer binder and geopolymer concrete, respectively when activated with an alkali which serves as an activator. Metakaolin, fly ash, and slag commonly used as aluminosilicate precursors in geopolymer formation are not always readily available worldwide. This has led to more intensive studies on readily available precursors. An example is a seashell which is part of the focus precursor of this study. Geopolymer binder aids in the reduction of CO_2 footprint to the atmosphere result of the greenhouse effect.

Aluminosilicates will either not react with water or do so slowly when put in an alkaline condition. However, these materials will hydrolyze and condense, producing new inorganic polymers with load-bearing capability [8]. Aluminosilicate materials are activated by applying alkalis. These alkalis are referred to as activators; examples include sodium hydroxide (NaOH), potassium hydroxide (KOH), sodium silicate (Na_2SiO_3), and potassium silicate (K_2SiO_3). The rate at which monomer (silicate and aluminate small molecules) dissolves is determined by the particle size of the precursors [8]. Some examples of aluminosilicate precursors are metakaolin, fly ash and slag.

Seashells are shells with a hard solid, protective outer layer known as an exoskeleton usually produced by a sea creature (mollusc) [4]. The shell is attached to the animal's body. Because of their infinite variety, seashells may be found worldwide. Their beauty, brilliant colours, and abundance along seashores are all aspects that contribute to their attraction [24,25]. Seashells are made of numerous layers of microstructures with varying mechanical characteristics, such as strength and toughness [4,26,27]. Many studies have investigated the properties, to find advantages in other areas. A seashell is primarily made of calcium carbonate or chitin and is the exoskeleton of an invertebrate (an animal without the need for a backbone). Most beach shells are the shells of marine molluscs, partially because such shells are composed of calcium carbonate, which lasts longer than chitin-based shells.

Clean and empty seashells left on beaches by waves and tides typically signify that the animal has passed away. According to Hung et al. [28], seashells are another widely available waste resource, with the majority being utilized for landfilling and just a tiny amount being reused for various applications such as handicrafts and fertilizers. The fisheries and aquaculture sectors create massive volumes of seashell trash yearly [21,29]. Seashells are also referred to as shells of marine molluscs which are marine species of bivalves (or clams), gastropods (or snails), scaphopods (or tusk shells), polyplacophorans (or chitons), and cephalopods (nautilus and spirula). These shells are mostly sold as decorative objects although bivalves and gastropods are mostly used as potential cementitious materials [30]. Gastropods and bivalves found in the sea are more abundant than those found on land or in freshwater in most cases [30]. Waste is generated from various kinds of seashells. In Asian countries like China and South Korea, Oyster shells are a significant waste agent and are highly challenging. It has been stated that for every 1 kg of oyster consumed, about 370–700 g of shell trash is created [31]. Each year, Peru produces over 25,000 tons of scallop shell debris, which when dumped in open areas pollutes the environment [4,32]. The amount of cockle shells collected in 2011 throughout Peninsular Malaysia's west coast, covering Pahang and Johor, is estimated by Malaysia's Department of Fisheries to have been about 57,544.40 tons [33]. In the building industry, seashells have been recycled in various ways for their properties.

More species of colourful, huge, shallow water-shelled marine molluscs exist in tropical and subtropical regions of the earth than in temperate areas and regions closer to the poles. Among marine shellfish species, bivalve molluscs are quite common. Approximately 87% of aquaculture (molluscan) is made up of bivalve molluscs, with clamshells making up 33.0%, oysters making up 31.3%, and mussels making up 12.1% [30].

Steel slag is a by-product of steel discharge via crude steel smelting. In a developing country like China, more than 100 million tons is being produced annually [34]. Steel slag in its raw state possesses clinker of low quality, low hydration and unstable chemical composition. However, cementitious components are produced through chemical modification and mechanical activation [35]. The major component of steel slag is CaO, SiO_2, Fe_2O_3 and Al_2O_3. Calcium oxide (CaO) is within range of 38%–48%, while SiO_2 ranges from 11% to 20%. The Si–Al components of steel slag are mostly mixed in the vitreous as (SiO_4) tetrahedrons, (AlO_4) tetrahedrons, or (AlO_6) coordination polyhedrons a due to the high temperature and fast cooling process. In the presence of an alkaline activator, the Si–O and Al–O bonds of the glass structure can be broken to produce amorphous glass or the network structure of aluminosilicate zeolite, which exhibits potential activity in geopolymerization [34,36]. The usual cement clinker minerals found in steel slag, however, exhibit hydration activity. Examples include tetra calcium aluminoferrite (C_4AF), tricalcium silicate (C_3S), and dicalcium silicate (C_2S) [37].

Cement clinker reactivity is superior to that of steel slag. Instead of being the primary raw material, steel slag would be ideal to be utilized as supplemental material to produce a geopolymer composite with excellent performance. Wang and Yan [37] study showed that low hydration activity of steel slag when sodium hydroxide solution stimulated the potential reactivity of sodium silicate. Zhang et al. [38] confirmed that excellent strength and better immobilization of heavy material are attained when 30% of steel slag powder is added and 70% of fly ash into an alkaline combination of NaOH, Na_2SiO_3 and water to synthesize geopolymer composite which certifies steel slag to be deployed as supplementary cementitious material converting waste to wealth. To the best of my knowledge, steel slag and seashell have not been investigated as source materials in the production of GPC, although the outstanding research in the production of geopolymer binder includes various aluminosilicate precursors and the activator, the essence of the study is this.

The goal of this study is to produce a geopolymer concrete synthesized by aluminosilicate precursors and activator. Seashell powder and steel slag were deployed as aluminosilicate precursors while sodium silicate gel (Na_2SiO_3) was used as an activator, the chemical composition of the precursors was examined via X-ray Fluorescence (XRF) analysis, and the mechanical property was examined after 3, 7, 14, 28 & 56 days ambient curing, characterization of the microstructural and mineralogical properties were examined via Scanning Electron Microscopy (SEM) and X-ray Diffraction (XRD) and thermal property of GPC was determined at 28 days. The need to develop a partial or total replacement for cement to mitigate the emission of greenhouse gases to the barest minimum and improve concrete's engineering properties cannot be over-emphasized therefore maximizing agro-industrial by-products as source materials for GPC is imperative.

2. Experimental programme

2.1. Materials

The seashell and steel slag, as shown in Fig. 1 (a) and (b), were obtained from Lagos beach and Top steel, Lagos. The seashell and steel slag were air-dried and pulverized with an abrasion machine at 1000 rev/min for 1 h at the Highway and Transportation Engineering Laboratory of Covenant University. Afterwards, they were sieved with a 75 μm sieve to obtain the finer particles as indicated in Fig. 1 (c) and (d). These were employed as the aluminosilicate precursors. Local suppliers delivered both the coarse and fine aggregate. Due to its cost-effectiveness and better pH activating characteristics, sodium silicate gel (Na_2SiO_3) was used as an activator. The specific gravity of the binders was examined via BS EN 196 -3 [39] guidelines deploying a specific gravity bottle and kerosene. The result reveals 3.4 g/cm^3, 2.37 g/cm^3, and 3.15 g/cm^3 for steel slag (SS), oyster seashell (OS) and Portland cement respectively.

2.2. Mix proportion

There is no specific design code for geopolymer concrete. However, the mix proportion was designed following American Concrete Institute [40]. The calculated quantity of each material (see Table 1): steel slag (SS), oyster seashell powder (OS), fine aggregate (FA), and coarse aggregate (CA) were mixed till a homogenous colour was attained. Then sodium silicate, Conplast-superplasticizer (SP) of 2% binder material by mass, and water were mixed, then added to the homogenous constituent, and mixed further at the temperature range of 26–28 $^{\circ}C$ until the GPC mix was consistent. The GPC fresh mix was cast into a mould of 100 × 100 × 100 mm^3, 100 mm diameter × 200 mm height, and 100 × 100 × 500 mm^3 then demoulded after 36 h for better polymerization and cured at the ambient temperature of 23 ± 5 $^{\circ}C$ and 65% relative humidity in accordance to BS EN 12390-2: 2019 [41] for a duration of 3, 7, 14, 28, and 56 days. The sodium silicate used had a pH value of 12.71, determined via a pH meter. To know if the activator possesses high alkalinity which facilitates geopolymerization and enhances strength [42,43]. Fig. 2 shows the mix design for Portland cement concrete (PCC), also the percentage replacement of seashell to slag was proportioned at 0%, 10%, 20%, and 30% to examine if the target strength will

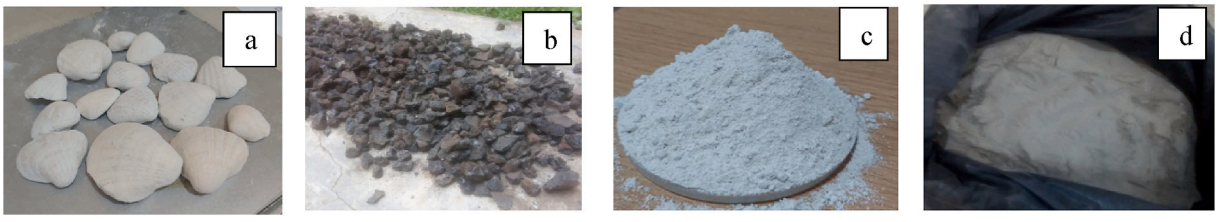

Fig. 1. (a) Oyster Seashell, (b) steel slag, (c) Oyster Seashell powder, and (d) Pulverized steel slag.

Table 1
Volumetric M 40 mix design for PCC & GPC.

	% Replacement			Mix design proportion (kg/m^3)							
Mix ID	PC	SS	OS	PC	SS	OS	FA	CA	Na_2SiO_3	SP	Water
PCC	100	0	0	452	0	0	762	1045	0	9.04	181.06
A	0	100	0	0	452	0	762	1045	133	9.04	57
B	0	90	10	0	407	45	762	1045	133	9.04	57
C	0	80	20	0	362	90	762	1045	133	9.04	57
D	0	70	30	0	316	136	762	1045	133	9.04	57

be attained for either structural or non-load bearing application.

2.3. Experimental test

2.3.1. X-ray fluorescence (XRF)

The chemical composition of the precursors, oyster seashell and steel were evaluated via a Phillips PW-1800 machineThe powdered seashell and slag samples were first ground for 60 s by 20 g each with 0.4 g of stearic acid to make pellets. The Gyro-mill was properly cleaned after each grinding to prevent contamination. The sample was transferred to the cup until it reached the level point after 1 g of stearic acid, which served as a binding agent, was weighed into an aluminium cup. The cup was then conveyed to Herzong pelletizing equipment after receiving through at 200 kN of pressure for 60 s. A sample holder on the x-ray equipment (Phillips PW-1800) was filled with the 2 mm pellets for analysis.

2.3.2. Slump test

The slump test was conducted in line with BS EN 123450-2 [44]. GPC fresh mix was filled into a metal cone mould of 100 mm internal diameter at the top, 200 mm diameter at the bottom and height of 300 mm. The cone opens at both ends. The cone will be filled at three stages and tamped with a rod of 600 mm long and 16 mm in diameter at each to ensure proper compaction. The cone was removed, and the tamping rod was placed on top to measure the distance of the fresh GPC to the tamping rod and taken as the slump value.

2.3.3. Mechanical tests

The mechanical was conducted via INSTRON 500R UTM for compressive strength test, split tensile strength test and flexural test in line with BS EN 12390-4 [45], BS EN 12390-6 [46], and BS EN 12390-5 [47] with the dimension of 100 × 100 × 100 mm cube, 100 mm diameter × 200 mm height cylinder and 100 × 100 × 500 mm beam respectively. The average value of two sample experimental tests was calculated and obtained.

2.3.4. Microstructural test

Scanning Electron Microscopy (SEM) machine Model 7000600 was deployed to analyse the Microstructural pattern present in the concrete sample at a hydration age of 28 days. The selected concrete PCC, A, B, C and D were magnified at 8000 to analyse the microstructural form.

2.3.5. XRD test

The mineralogical phase of the selected concrete samples, A, B and PCC was evaluated after 28 days of hydration via Rigaku D/Max-lllC X-ray diffractometer machine. The samples were sieved to 0.074 mm and pelletized. They were then collected in a 35 mm × 50 mm aluminium alloy grid on a flat glass plate, coated with paper. By gently pressing the samples using gloved hands, the samples were compacted. Deploying CuKα radiation set at 40 kV and 20 mA, samples were scanned at a rate of 2°/min between 2 and

Fig. 2. Geopolymer concrete fresh mix.

80° at room temperature.

2.3.6. Thermal conductivity and resistivity test

A test for thermal conductivity was conducted to evaluate the material's thermal conductivity and storage via the TD 1002 heat conduction base unit machine as shown in Fig. 3 (a). The thermal conductivity test is determined via Eq. (i), per Fourier's law and measured in watts per meter kelvin (W/mK). The samples were cast into a cylindrical mould of 30 mm diameter × 20 mm height as shown in Fig. 3 (b). The Q-value was set at 9.9W for 10 min, and the temperature reading was taken in Celsius and then converted to Kelvin as shown in Fig. 3 (c). The thermal resistivity test determines the resistance of a sample to heat flow. Thermal resistivity is the reciprocal of thermal conductivity measured in kelvin meters per watt. (Km/W).

$$k = \frac{xQ}{A\Delta T} \tag{i}$$

where Q = heat quantity which flows through the sample; x = sample thickness; A = sample surface area; k = sample thermal conductivity; Δand T = change in temperature.

2.3.7. Drying shrinkage test

A test for drying shrinkage was conducted in alignment with ASTM C 596 [48] on the sample beams, 50 mm × 50 mm × 250 mm, which were stored at ambient temperature. It is determined via Eq. (ii).

$$\text{Dry Shrinkage } \% = \frac{L_1 - L_2}{G} \times 100\% \tag{ii}$$

where, L_1 = extrusion length; L_2 = length obtained after curing; G = Gauge length, at a constant value of 250 mm.

3. Results and discussion

3.1. X-ray fluorescence (XRF) analysis

Fig. 4 (a)-(c) show the results of chemical compositions of binders used in this study. The results of steel slag, as shown in Fig. 4 (a), did not satisfy all the requirements as stipulated in BS EN 15167-1 [49] for a supplementary cementitious material where $(CaO + MgO/SiO_2) \geq 1$, $(CaO/SiO_2) \leq 1.4$, $SiO_2 + CaO + MgO \geq 67\%$. But the oyster seashell powder in Fig. 4 (b) complied with the specifications. Also, Portland cement in Fig. 4 (c) satisfied the requirement of BS EN 192-2 [50], where CaO, SiO_2, Al_2O_3 and Fe_2O_3 are within the range of 61–69%, 18–24%, 2.6–8% and 1.5–7% respectively.

3.2. Slump test

The experimental result in Fig. 5 indicated that fresh GPC mix composed of 100% slag possessed high viscosity, resulting in low workability, while the increment in seashell replacement increases the workability, which is attributed to its lower specific gravity than that of slag which aligns with Nath and Sarker [51] and Oyebisi et al. [2] that percentage replacement of material with lower specific gravity increase workability which in turn increases slump value. However, Portland cement concrete exhibited a high slump value which is attributed to its specific gravity, although seashells possessed a lower specific gravity than PCC, which was meant to result in a higher slump value but has low percentage composition combined with steel slag in the concrete mix resulting in low slump value. Also, the consistency increase of GPC with seashell replacement increase can be attributed to interfacial particle reduction percentage of steel slag which results in a slump value increase [43]. Due to the low slump result obtained for all GPC samples, application of fresh concrete must be with vibration because it is less than 50 mm–150 mm while that of PCC can be applied without vibration because it is within the range of 50 mm–150 mm [43,44].

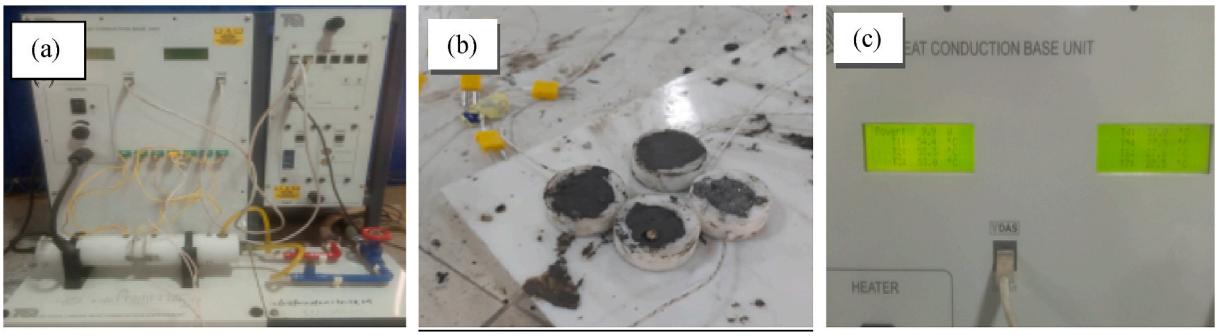

Fig. 3. (a) Sample, (b) Displayed thermal readings, (c) TD 1002 heat conduction base unit.

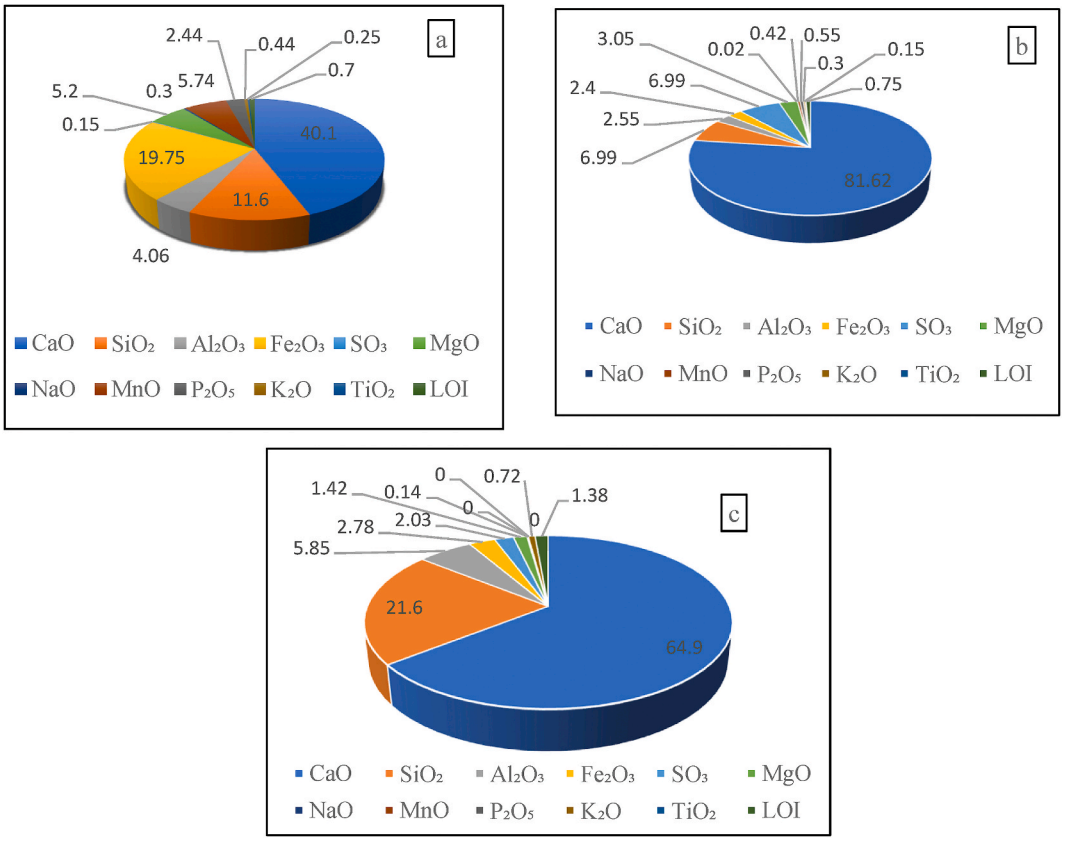

Fig. 4. Chemical compositions of (a) Pulverized steel slag, (b) Oyster seashell powder, and (c) PLC.

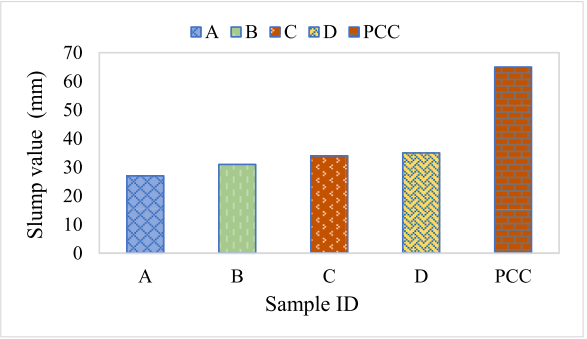

Fig. 5. Fresh concrete mix slump value.

3.3. Mechanical tests

3.3.1. Compressive strength test

A test on compressive strength was done on 100 × 100 × 100 mm^3 hardened concrete on 3, 7, 14, 28, and 56 ambient curing days for GPC and water curing for PCC via machine model INSTRON 500R UTM. The optimum compressive strength was attained at 10% seashell replacement and 90% slag obtained a value of 21.75 & 22.19 N/mm^2 at 28 and 56 days. However, PCC attained a greater compressive strength of 41.35 and 42.177 N/mm^2 at 28 and 56 days respectively, which can be attributed to the chemical composition content of Portland cement majorly in calcium oxide (CaO), silicon dioxide (SiO_2) & aluminium oxide (Al_2O_3) high percentage Fig. 6 displays the compressive strength for sample curing days. Optimum GPC strength was attained at 10% of seashell-powder addition. Seashell replacement exceeding 10% resulted in strength declination, similar to Yang and Jang [52]. However, their study was on calcined seashells, the optimum compressive strength was attained at 5% of calcined seashell replacement and gradual strength declination exceeded 5%. Oyster seashells possess a high percentage content in CaO and a low percentage content in SiO_2 & Al_2O_3

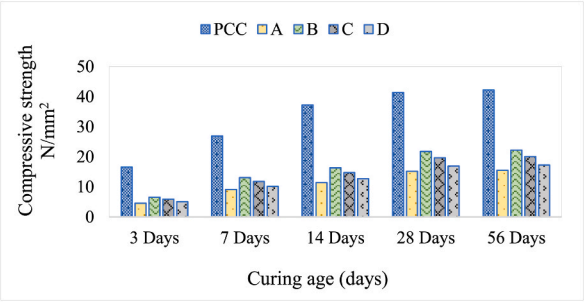

Fig. 6. Compressive strength results.

while steel slag possessed a satisfactory percentage content of CaO and a low percentage content in SiO_2 & Al_2O_3 but higher than seashell which can be attributed for the strength of GPC attained.

3.3.2. *Splitting tensile strength*

A test on splitting tensile was performed to evaluate the tensile strength of concrete via a 100 mm × 200 mm high cylinder of concrete, which split across the vertical diameter by the exertion of a load until it collapsed. Fig. 7 shows GPCs tensile strength before the collapse at 3, 7, 14, 28, and 56 days. Sample B has an optimum strength for 3, 7, 14, 28, and 56 days for GPC. Portland cement concrete exhibited higher strength than GPC. The split tensile strength increased with an increase in compressive strength, which is in alignment with Neville [53] and Oyebisi et al. [43] with increasing compressive strength, split tensile strength also increases. The higher strength exhibited by PCC can be attributed to the satisfactory chemical composition present in Portland cement as stipulated by Ref. [50], also from the XRD analysis, PCC possessed high CaO intensity than that of GPC yielding better concrete hardness, thus higher performance and better splitting tensile strength. Sample B (90% slag, 10% seashell) exhibited better performance than the rest GPC samples due to less pores more microstructural integration as revealed in the SEM micrograph.

3.3.3. *Flexural strength test*

A one-point flexural test was conducted on a beam of 100 × 100 × 500 mm to estimate the bending resistance of an unreinforced concrete beam. Fig. 8 displays the flexural strength of PCC and GPC at various curing days. Sample B attained optimum strength for GPC. However, PCC attained the optimum concrete strength which can be attributed to its chemical oxide composition content. A similar trend was observed as compressive strength increases flexural strength also increased, which is in alignment with Neville [53] and Oyebisi [43]. The strength the material attained before yielding to bending can be attributed to the hardening and bonding of the material in hydration. The excellent bonding and hardening are dependent on the material reactivity and the content of oxide composition it possesses.

3.4. *Microstructural analysis*

The Scanning Electron Microscopy (SEM) micrograph with an accelerated voltage of 20 kV magnified at 8000 reveals the microstructures of GPC produced. The results are presented in Fig. 9 (a)-(d). A 100% pulverized steel slag, as shown in Fig. 9 (a), possessed an amorphously flake form with a little disintegration, which resulted in low strength. Fig. 9 (b) (90% pulverized steel slag and 10% oyster seashell powder) possessed amorphous structure with traces of spikes, better integration with fewer pores which support the better strength attained for GPC. An 80% steel slag and 20% oyster shell powder as indicated in Fig. 9 (c), revealed an amorphous needle like structure, while the sample presented in Figs. 9 (d), 70% steel slag and 20% oyster shell powder, showed little traces of spherical form. The increment of seashell led to an increase in void as revealed in Fig. 9 (c) and (d). This aligns with similar

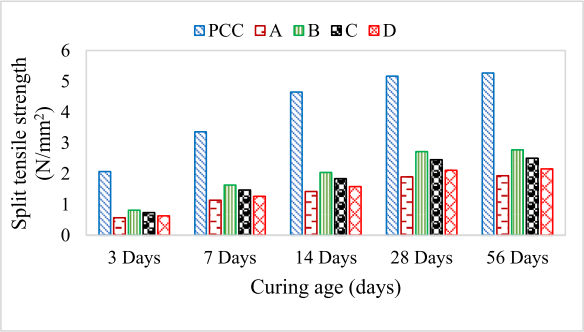

Fig. 7. Split tensile strength results.

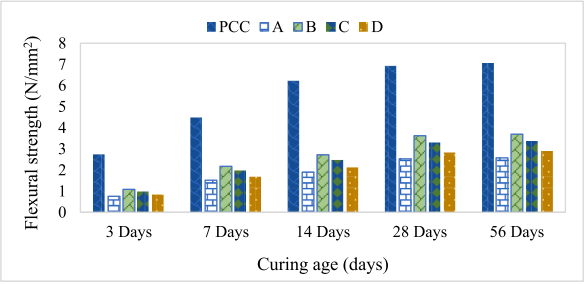

Fig. 8. Flexural strength results.

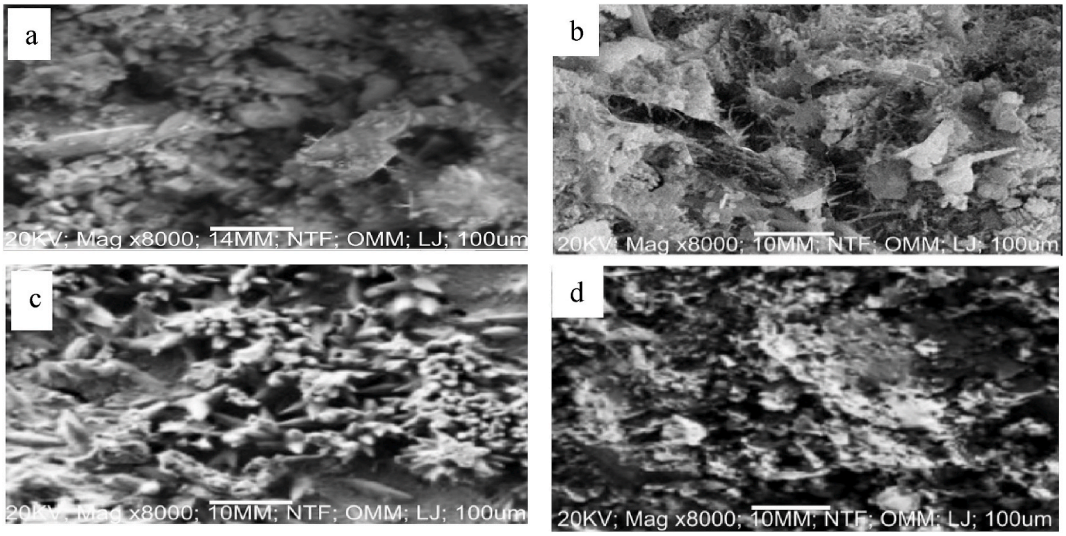

Fig. 9. As received SEM analysis for (a) Sample A, (b) Sample B, (c) Sample C, and (d) Sample D.

study where an increment in oyster shell powder increased the void content of one-part alkali activated concrete [52].

3.5. X-ray diffraction (XRD)

The X-ray diffraction results of the GPC produced, which displayed the least and best mechanical strengths, are shown in Fig. 10 (a) and (b). Similarly, Fig. 10 (c) displays the Portland cement concrete's XRD results. A scan range of 5–80° along two theta angles was used for the analysis. The analysis depicts calcium silicate (CS), calcium hydroxide (CH), quartz (Si), Ettringite (E) and calcium oxide (CaO), which enhance the mechanical properties of concrete. Calcium hydroxide enhances mechanical strength and its form by the synthesis of calcium oxide (CaO) with water (H_2O) during hydration. Quartz yields hardness to concrete and is contained in the aggregate component that makes up the concrete. Ettringite helps in fast hydration, dry shrinkage reduction, and improves strength. Calcium is depicted in hydrated and pure form as calcium hydroxides and calcium oxide in the Portland cement concrete which aids in hardened network and birth excellent strength [43]. The high intensity of CaO present in the Portland cement concrete is attributed to better mechanical strength than GPC. Samples A and B, as shown in Fig. 9 (a) and (b), exhibited a sharp peak of CH due to the cementitious reaction present in GPC as aligned with Oyebisi et al. [42]. The quartz peak is due to aggregate mix [43]. The compound ingredients in 90% pulverized steel slag and 10% oyster seashell powder in Fig. 10 (b) displayed higher intensity than in 100% pulverized steel slag in Fig. 10 (a), which may be attributable to an increase in strength.

3.6. Thermal conductivity and resistivity test

A thermal conductivity test was conducted via a TD 1002 HEAT CONDUCTION BASE UNIT MACHINE on the sample compositions, PCC, sample A (100% slag), sample B (90% slag, 10% seashell) and sample C (80% slag, 20% seashell). Samples were cast into a cylindrical mould of 30 mm diameter × 20 mm height. A Q-value was set at 9.9 W for 10 min, and the temperature reading was taken in Celsius and then converted to Kelvin. Sample C (80% slag, 20% seashell) obtained the least thermal conductivity value of 13.60 W/mK, preceded by 13.81 W/mK, of Portland cement concrete (PCC). Sample A obtained the highest value of 17.65 W/mK indicating greater heat conduction than the rest samples, which has a downside in applying high temperate regions. The result obtained in sample C

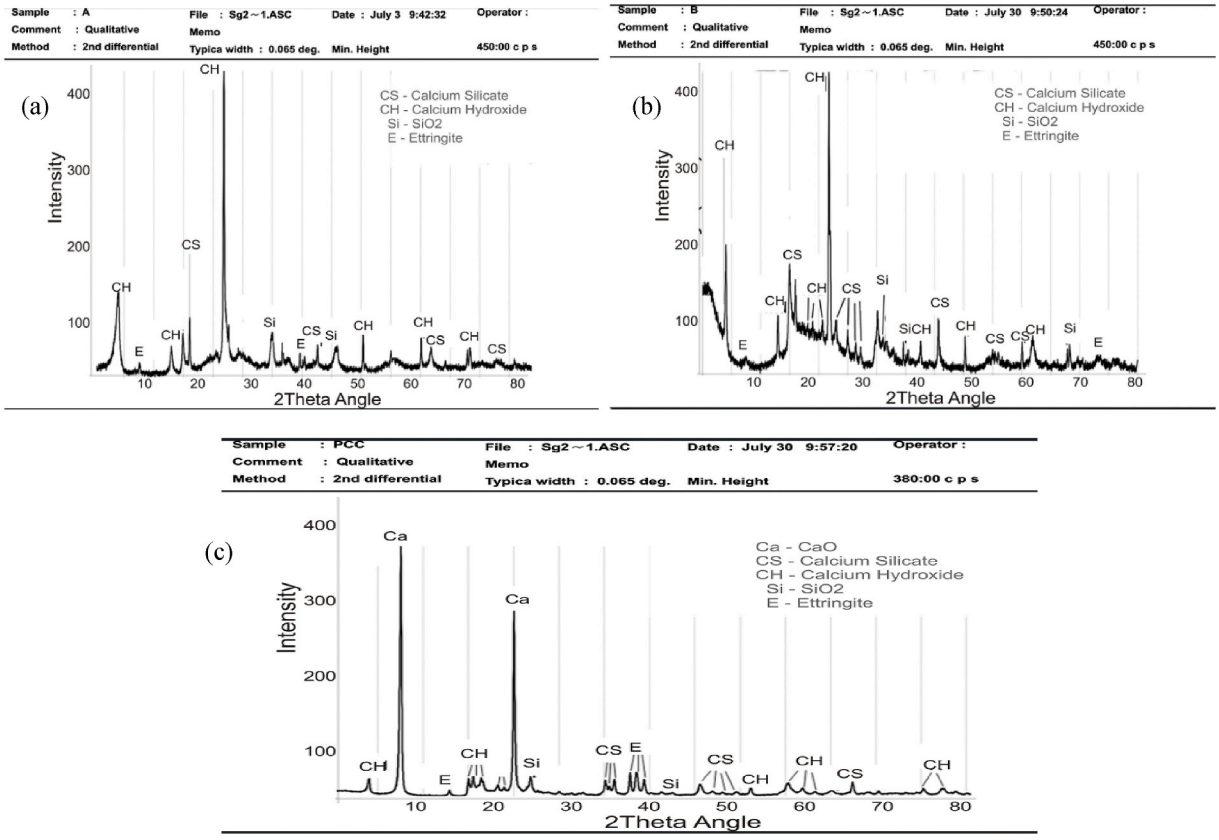

Fig. 10. As received XRD results for (a) Sample A, (b) Sample B, and (c) PCC.

implies that increments in a seashell decrease the thermal conductivity rate. Increment in 20% seashell replacement attained lower thermal conductivity than PCC, implying better thermal insulation. As shown in Fig. 11 (a) seashell increment attains low conductivity in line with [4], improving thermal insulation. Low specific gravity material possesses low thermal conductivity. This aligns with the findings of Kodur and Khaliq [54] and Oyebisi et al. [55] that low thermal conductivity of concrete is attributed to the percentage increment of material with lower specific gravity. In their study, pozzolan material increment yields low thermal conductivity which improves the thermal insulating property. However, this study did not implement pozzolan material.

Thermal resistivity is the reciprocal of thermal conductivity which implies that the optimum resistivity value was obtained at sample C (80% slag, 20% seashell) indicating a better insulator against heat than the other samples, as shown in Fig. 11 (b) which is an added advantage deployed in high temperate regions. Sample A (100% slag) obtained the lowest resistivity, which reveals the sample as the least insulating material against heat compared to the rest samples.

3.7. Drying shrinkage test

Fig. 12 displays the percentage shrinkage of the GPC and PCC samples. A drying shrinkage test was conducted on samples cured for 1–56 days at an ambient temperature range of 26–28 $^{\circ}C$ for GPC and PCC beams. PCC obtained the highest shrinkage value for concrete for all curing days this can be attributed to the ambient curing method applied. As shown in Fig. 12, sample A (100% slag) and B (90% slag, 10% seashell) attained the highest percentage shrinkage value of 0.42 for GPC at 28 days and 0.472 & 0.464 at 56 days respectively, indicating they expelled more water than C (80% slag, 20% seashell) and D (70% slag, 30% seashell) which attained low percentage value of 0.32 & 0.20 for GPC at 28 days and 0.400 and 0.360 at 56 days respectively. Therefore, seashell increments yield less shrinkage. According to Bamigboye et al. [24] and Eo and Yi [56], the value of shrinking decreases as seashell content in the concrete mix increases. In addition, the findings of this study support those of a prior study that found that adding more seashells to cement mortar reduced dry shrinkage [57].

4. Conclusions

This study examines the mechanical, characterization, thermal and durability properties of GPC synthesized from a seashell, steel slag, and sodium silicate. Based on the experimental findings, the following conclusions were drawn:

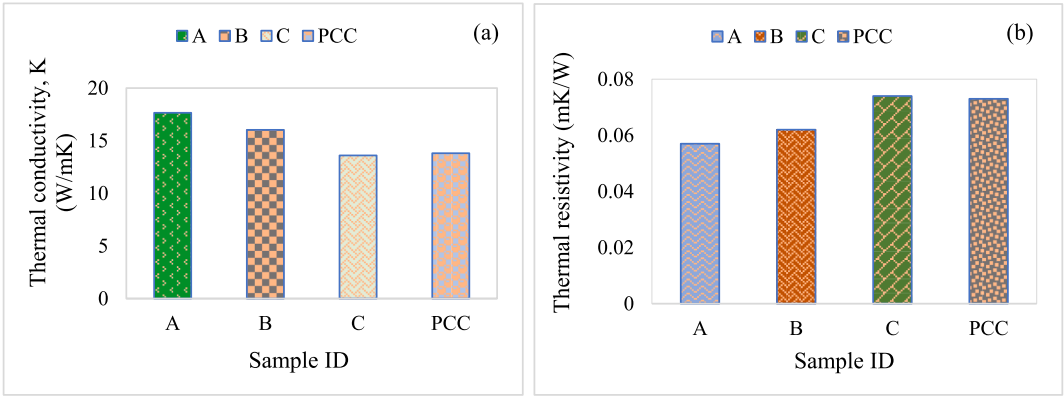

Fig. 11. (a) Thermal conductivity of sample composition, (b) Thermal resistivity of sample composition.

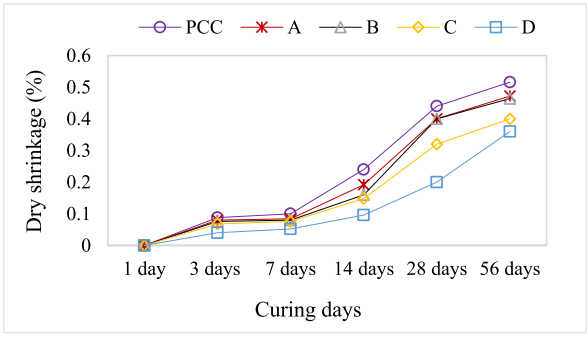

Fig. 12. Dry shrinkage for GPC and PCC.

i) The optimum mechanical strength was attained at 10% oyster seashell powder replacement and 90% pulverized steel slag for GPC, however, PCC exhibited better mechanical strength.
ii) A 20% seashell replacement in steel slag-seashell powder-based GPC attained lower conductivity than Portland cement.
iii) Seashell increment yields less shrinkage at 20% and 30% replacement. However, PCC attained higher shrinkage value which can be attributed to ambient curing method applied.
iv) The SEM images reveal an amorphous structure with less void and compaction of GPC. However, 90% pulverized steel slag and 10% oyster seashell powder exhibited better compaction with fewer voids.
v) The XRD study shows that PCC has a higher CaO content than GPC, creating a hardened network that increases the strength of concrete. .
vi) Steel slag-seashell powder-based geopolymer concrete is satisfactory only as non-loading bearing concrete or mass concrete.
vii) The geopolymer binder synthesized from steel slag-seashell powder and sodium silicate can be applied as walling materials in hot temperature regions due to their better thermal insulating properties at 20% seashell replacement.

The benefits of this study to future research are as follows: it converts waste to wealth by utilizing the by-products as a binding construction material which can be applied for concrete and mortars in this case oyster seashell and steel slag activated with sodium silicate; it contributes to the attainment of thermal insulating materials, making buildings more comfortable for the dwellers in hot temperate regions based on the thermal conductivity result obtained especially at 20% seashell replacement blended with steel slag. However, it should be adopted as a walling and non-loading bearing material due to the experimental mechanical result obtained.

Author contribution statement

Wilson Chukwunonyenim Okoro: Conceived and designed the experiments; Performed the experiments; Analyzed and interpreted the data; Contributed reagents, materials, analysis tools or data; Wrote the paper.

Solomon Oyebisi: Conceived and designed the experiments; Analyzed and interpreted the data; Contributed reagents, materials, analysis tools or data; Wrote the paper.

Funding statement

This research was financially supported by the Covenant University Centre for Research, Innovation and Discovery.

Data availability statement

Data will be made available on request.

Declaration of interest's statement

The authors declare no conflict of interest.

Acknowledgement

The researchers express their gratitude to the Covenant University Centre for Research, Innovation, and Discovery (CUCRID) for providing conducive environment for this study.

References

[1] F. Farooq, et al., Geopolymer concrete as sustainable material: a state of the art review, Construct. Build. Mater. 306 (September) (2021), 124762, https://doi.org/10.1016/j.conbuildmat.2021.124762.
[2] S. Oyebisi, J. Akinmusuru, A. Ede, O. Ofuyatan, 14 Molar Concentrations of Alkali-Activated Geopolymer Concrete 14 Molar Concentrations of Alkali-Activated Geopolymer Concrete, 2018, https://doi.org/10.1088/1757-899X/413/1/012065.
[3] A. Hasnaoui, A. Bourguiba, Y. El Mendili, N. Sebaibi, M. Boutouil, A preliminary investigation of a novel mortar based on alkali-activated seashell waste powder, Powder Technol. 389 (2021) 471–481, https://doi.org/10.1016/j.powtec.2021.05.069.
[4] G.O. Bamigboye, A.T. Nworgu, A.O. Odetoyan, M. Kareem, D.O. Enabulele, D.E. Bassey, Sustainable use of seashells as binder in concrete production : prospect and challenges, J. Build. Eng. 34 (2021), 101864, https://doi.org/10.1016/j.jobe.2020.101864. July 2020.
[5] Z. Podolsky, J. Liu, H. Dinh, J.H. Doh, M. Guerrieri, S. Fragomeni, Case Studies in Construction Materials State of the art on the application of waste materials in geopolymer concrete, Case Stud. Constr. Mater. 15 (April) (2021), e00637, https://doi.org/10.1016/j.cscm.2021.e00637.
[6] W. Shanks, C.F. Dunant, M.P. Drewniok, R.C. Lupton, A. Serrenho, J.M. Allwood, Resources , Conservation & Recycling How much cement can we do without, Lessons from cement material fl ows in the UK 141 (2019) 441–454, https://doi.org/10.1016/j.resconrec.2018.11.002. November 2018.
[7] L. Imtiaz, S.K. Ur Rehman, S.A. Memon, M.K. Khan, M.F. Javed, A review of recent developments and advances in eco-friendly geopolymer concrete, Appl. Sci. 10 (21) (2020) 1–56, https://doi.org/10.3390/app10217838.
[8] A.L. Almutairi, B.A. Tayeh, A. Adesina, H.F. Isleem, A.M. Zeyad, Potential applications of geopolymer concrete in construction: a review, Case Stud. Constr. Mater. 15 (September) (2021), e00733, https://doi.org/10.1016/j.cscm.2021.e00733.
[9] A.M. Zeyad, H.M. Magbool, B.A. Tayeh, A.R. Garcez de Azevedo, A. Abutaleb, Q. Hussain, Production of geopolymer concrete by utilizing volcanic pumice dust, Case Stud. Constr. Mater. 16 (2022), e00802, https://doi.org/10.1016/j.cscm.2021.e00802. September 2021.
[10] B.A. Tayeh, A.M. Zeyad, I.S. Agwa, M. Amin, Effect of elevated temperatures on mechanical properties of lightweight geopolymer concrete, Case Stud. Constr. Mater. 15 (2021), e00673, https://doi.org/10.1016/j.cscm.2021.e00673. July.
[11] M.S. Saif, M.O.R. El-Hariri, A.I. Sarie-Eldin, B.A. Tayeh, M.F. Farag, Impact of Ca+ content and curing condition on durability performance of metakaolin-based geopolymer mortars, Case Stud. Constr. Mater. 16 (2022), e00922, https://doi.org/10.1016/j.cscm.2022.e00922. February.
[12] S.M.A. Qaidi, B.A. Tayeh, A.M. Zeyad, A.R.G. de Azevedo, H.U. Ahmed, W. Emad, Recycling of mine tailings for the geopolymers production: a systematic review, Case Stud. Constr. Mater. 16 (2022), e00933, https://doi.org/10.1016/j.cscm.2022.e00933. February.
[13] B.A. Tayeh, A. Hakamy, M. Amin, A.M. Zeyad, I.S. Agwa, Effect of air agent on mechanical properties and microstructure of lightweight geopolymer concrete under high temperature, Case Stud. Constr. Mater. 16 (2022), e00951, https://doi.org/10.1016/j.cscm.2022.e00951. February.
[14] S.M.A. Qaidi, B.A. Tayeh, H.F. Isleem, A.R.G. de Azevedo, H.U. Ahmed, W. Emad, Sustainable utilization of red mud waste (bauxite residue) and slag for the production of geopolymer composites: a review, Case Stud. Constr. Mater. 16 (2022), e00994, https://doi.org/10.1016/j.cscm.2022.e00994. February.
[15] T. Phoo-Ngernkham, A. Maegawa, N. Mishima, S. Hatanaka, P. Chindaprasirt, Effects of sodium hydroxide and sodium silicate solutions on compressive and shear bond strengths of FA-GBFS geopolymer, Construct. Build. Mater. 91 (2015) 1–8, https://doi.org/10.1016/j.conbuildmat.2015.05.001.
[16] E. Adesanya, K. Ohenoja, T. Luukkonen, P. Kinnunen, M. Illikainen, One-part geopolymer cement from slag and pretreated paper sludge, J. Clean. Prod. 185 (2018) 168–175, https://doi.org/10.1016/j.jclepro.2018.03.007.
[17] J. Zhang, H. Chen, T. Mu, Y. Pan, Research and application of shell powder, IOP Conf. Ser. Earth Environ. Sci. 170 (3) (2018) 1–5, https://doi.org/10.1088/1755-1315/170/3/032031.
[18] B.A. Tayeh, M.W. Hasaniyah, A.M. Zeyad, M.O. Yusuf, Properties of concrete containing recycled seashells as cement partial replacement: a review, J. Clean. Prod. 237 (2019), 117723, https://doi.org/10.1016/j.jclepro.2019.117723.
[19] A. Hasan-Ghasemi, M. Nematzadeh, H. Fallahnejad, Post-fire residual fracture characteristics and brittleness of self-compacting concrete containing waste PET flakes: experimental and theoretical investigation, Eng. Fract. Mech. 261 (2022), 108263, https://doi.org/10.1016/j.engfracmech.2022.108263. January.
[20] M. Nematzadeh, A. Baradaran-Nasiri, M. Hosseini, Effect of pozzolans on mechanical behavior of recycled refractory brick concrete in fire, Struct. Eng. Mech. 72 (2019) 339–354.
[21] C.M. Moffitt, L. Cajas-Cano, Blue growth: the 2014 FAO state of the world fisheries and aquaculture, Fisheries 39 (11) (2014) 552–553, https://doi.org/10.1080/03632415.2014.966265.
[22] G.O. Bamigboye, et al., Waste materials in highway applications: an overview on generation and utilization implications on sustainability, J. Clean. Prod. 283 (2021), 124581, https://doi.org/10.1016/j.jclepro.2020.124581.
[23] M. Nematzadeh, A. Maghferat, M.R. Zadeh Herozi, Mechanical properties and durability of compressed nylon aggregate concrete reinforced with Forta-Ferro fiber: experiments and optimization, J. Build. Eng. 41 (2021), 102771, https://doi.org/10.1016/j.jobe.2021.102771. March.
[24] G. Bamigboye, D. Enabulele, A.O. Odetoyan, M.A. Kareem, A. Nworgu, D. Bassey, Mechanical and durability assessment of concrete containing seashells: a review, Cogent Eng. 8 (1) (2021), https://doi.org/10.1080/23311916.2021.1883830.
[25] M. Neamitha, A. Muthadhi, Performance of pervious concrete with industrial waste as coarse aggregate – an overview, Int. J. Emerging. Technol. Adv Eng. 6 (9) (2016) 155–161.
[26] V. Gadgihalli, R. Prasad, H. Dinakar, ANALYSIS OF PROPERTIES OF CONCRETE USING SEA SHELLS, vol. 5, 2017, pp. 374–378, https://doi.org/10.5281/zenodo.1117283.
[27] A.M. Zeyad, B.A. Tayeh, M.O. Yusuf, Strength and transport characteristics of volcanic pumice powder based high strength concrete, Construct. Build. Mater. 216 (2019) 314–324, https://doi.org/10.1016/j.conbuildmat.2019.05.026.

[28] K. Hung, U.J. Alengaram, M. Zamin, S. Cheng, W. Inn, C. Wah, Recycling of seashell waste in concrete : a review, Construct. Build. Mater. 162 (2018) 751–764, https://doi.org/10.1016/j.conbuildmat.2017.12.009.
[29] W.A.S. Bin Wan Mohammad, N.H. Othman, M.H. Wan Ibrahim, M.A. Rahim, S. Shahidan, R.A. Rahman, A review on seashells ash as partial cement replacement, IOP Conf. Ser. Mater. Sci. Eng. 271 (1) (2017), https://doi.org/10.1088/1757-899X/271/1/012059.
[30] G.O. Bamigboye, O. Okara, D.E. Bassey, K.J. Jolayemi, D. Ajimalofin, The use of Senilia senilis seashells as a substitute for coarse aggregate in eco-friendly concrete, J. Build. Eng. 32 (September) (2020), 101811, https://doi.org/10.1016/j.jobe.2020.101811.
[31] Z. Yao, M. Xia, H. Li, T. Chen, Y. Ye, H. Zheng, Bivalve shell: not an abundant useless waste but a functional and versatile biomaterial, Crit. Rev. Environ. Sci. Technol. 44 (22) (2014) 2502–2530, https://doi.org/10.1080/10643389.2013.829763.
[32] C. Varhen, S. Carrillo, G. Ruiz, Experimental investigation of Peruvian scallop used as fine aggregate in concrete, Construct. Build. Mater. 136 (2017) 533–540, https://doi.org/10.1016/j.conbuildmat.2017.01.067.
[33] M. Azmi, M. Johari, Cockle shell ash replacement for cement and filler in concrete, Malaysian J. Civ. Eng. 25 (2) (2013) 201–211, https://doi.org/10.11113/mjce.v25n2.303.
[34] X. Zhu, W. Li, Z. Du, S. Zhou, Y. Zhang, F. Li, Recycling and utilization assessment of steel slag in metakaolin based geopolymer from steel slag by-product to green geopolymer, Construct. Build. Mater. 305 (August) (2021), 124654, https://doi.org/10.1016/j.conbuildmat.2021.124654.
[35] Y.N. Dhoble, S. Ahmed, Review on the innovative uses of steel slag for waste minimization, J. Mater. Cycles Waste Manag. 20 (3) (2018) 1373–1382, https://doi.org/10.1007/s10163-018-0711-z.
[36] L. Kriskova, et al., Effect of mechanical activation on the hydraulic properties of stainless steel slags, Cement Concr. Res. 42 (6) (2012) 778–788, https://doi.org/10.1016/j.cemconres.2012.02.016.
[37] Q. Wang, P. Yan, Hydration properties of basic oxygen furnace steel slag, Construct. Build. Mater. 24 (7) (2010) 1134–1140, https://doi.org/10.1016/j.conbuildmat.2009.12.028.
[38] T. Zhang, Q. Yu, J. Wei, J. Li, Investigation on mechanical properties, durability and micro-structural development of steel slag blended cements, J. Therm. Anal. Calorim. 110 (2) (2012) 633–639, https://doi.org/10.1007/s10973-011-1853-6.
[39] BS EN 196-3, British Standard EN 196-3, Method of Testing Cement: Physical Test, BSI, London, 2016.
[40] ACI 211.1-91, *Standard Practices for Selecting Proportions for Normal, Heavyweight and Mass Concrete*, 2002.
[41] B.S. EN 12350-8, BSI standards publication testing hardened concrete, Br. Stand. 18 (April) (2019).
[42] S. Oyebisi, A. Ede, F. Olutoge, D. Olukanni, Assessment of activity moduli and acidic resistance of slag-based geopolymer concrete incorporating pozzolan, Case Stud. Constr. Mater. 13 (2020), e00394, https://doi.org/10.1016/j.cscm.2020.e00394.
[43] S. Oyebisi, A. Ede, F. Olutoge, D. Omole, Geopolymer concrete incorporating agro-industrial wastes : effects on mechanical properties , microstructural behaviour and mineralogical phases, Construct. Build. Mater. 256 (2020), 119390, https://doi.org/10.1016/j.conbuildmat.2020.119390.
[44] BS EN 12350-2, Testing Fresh Concrete, Slump-test , British Standards Institution - Publication Index | NBS," *thenbs.com*, 2009 accessed Mar. 05, 2022), https://www.thenbs.com/PublicationIndex/Documents/Details?DocId=288976.
[45] B.S. EN, British Standard EN 12390- 4, Testing Hardened Concrete: Compressive Strength of Test Specimens, BSI, London, 2019, 12390-4.
[46] B.S. EN, British Standard EN 12390-6, Testing Hardened Concrete: Splitting Tensile Strength of Test Specimens, BSI, London, 2019, 12390-6.
[47] B.S. EN, British Standard EN 12390 -5, Testing Hardened Concrete: Flexural Strength of Test Specimens, BSI, London, 2019, 12390-5BSI: London, 2019.
[48] ASTM C 596, Standard Test Method for Drying Shrinkage of Mortar Containing Hydraulic Cement 1, vol. 2, American Society for Testing and Materilas, 2001, p. 4.
[49] BS EN 15167-1, BS EN 15167-1:2006 Ground granulated blast furnace slag for use in concrete, mortar and grout Definitions, specifications and conformity criteria - European Standards," *.en-standard*.eu. https://www.en-standard.eu/bs-en-15167-1-2006-ground-granulated-blast-furnace-slag-for-use-in-concrete-mortar-and-grout-definitions-specifications-and-conformity-criteria/, 2006 accessed Aug. 01, 2022.
[50] BS EN 192-2, British Standard EN 196-2, Methods of Testing Cement: Chemical Analysis of Cement, BSI, London, 2016.
[51] P. Nath, P.K. Sarker, Effect of GGBFS on setting, workability and early strength properties of fly ash geopolymer concrete cured in ambient condition, Construct. Build. Mater. 66 (2014) 163–171, https://doi.org/10.1016/j.conbuildmat.2014.05.080.
[52] B. Yang, J.G. Jang, Environmentally benign production of one-part alkali-activated slag with calcined oyster shell as an activator, Construct. Build. Mater. 257 (2020), https://doi.org/10.1016/j.conbuildmat.2020.119552.
[53] A.M. Neville, Properties of Conrete, FIFTH. Pearson Education Ltd, England, 2011.
[54] V. Kodur, W. Khaliq, Effect of temperature on thermal properties of different types of high-strength concrete, J. Mater. Civ. Eng. 23 (6) (2011) 793–801, https://doi.org/10.1061/(asce)mt.1943-5533.0000225.
[55] S. Oyebisi, A. Ede, F. Olutoge, H. Owamah, T. Igba, Slag-based geopolymer concrete incorporating ash: effects on thermal performance, Aust. J. Civ. Eng. (2021) 1–14, https://doi.org/10.1080/14488353.2021.1953234, 0000.
[56] S.-H. Eo, S.-T. Yi, Effect of oyster shell as an aggregate replacement on the characteristics of concrete, Mag. Concr. Res. 67 (15) (2015) 833–842, https://doi.org/10.1680/macr.14.00383.
[57] H.Y. Wang, W. Ten Kuo, C.C. Lin, C. Po-Yo, Study of the material properties of fly ash added to oyster cement mortar, Construct. Build. Mater. 41 (2013) 532–537, https://doi.org/10.1016/j.conbuildmat.2012.11.021.